Grazing-incidence x-ray-scattering study of (001)-oriented high-quality epitaxial Co/Cr superlattices

N. Metoki, W. Donner, and H. Zabel
Fakultät für Physik und Astronomie, Institut für Experimentalphysik (Festkörperphysik), Ruhr-Universität Bochum, D-44780 Bochum, Federal Republic of Germany
(Received 18 October 1993; revised manuscript received 18 January 1994)

The structural properties of Co/Cr(001) superlattices grown by molecular-beam epitaxy have been studied by means of grazing-incidence x-ray-scattering techniques. From the in-plane diffraction pattern, we find that hcp-Co(11.0) is epitaxially grown on Cr(001) with the Co[00.1] axis parallel to Cr[110]. This epitaxial relation is equivalent to the Pitsch-Schrader orientational relationship. The Co layers exhibit a precursive structural phase transition from hcp to bcc with decreasing Co layer thickness t_{Co}. First, the Co in-plane unit cell changes its shape from rectangular (hcp) to square (bcc), due to the epitaxial strain. Second, the intensity I of the hcp-Co$\{\bar{1}1.1\}$ spots shows a continuous decrease with decreasing t_{Co}. The intensity I is proportional to the square of the displacement δ of the Co atoms from the bcc center sites, which is the order parameter for this structural transition. This intensity decrease therefore implies that the Co lattice continuously changes its symmetry from hcp to bcc. The experimentally determined t_{Co} dependence of δ is in good agreement with a model calculation describing the competition of the surface potential on Cr(001) and the bulk hcp potential of Co. Finally, we find that the observed anomalous out-of-plane expansion of the Co layers is a precursor of the structural transition. The non-Poisson-like behavior can be explained by a rigid-atom model which takes into account the atomic displacement during the structural transition.

I. INTRODUCTION

Magnetic metal multilayers and superlattices have attracted much interest in recent years both for fundamental studies in magnetism and for their potential applications as magneto-optical storage devices and as magnetic sensors.[1] Recent important discoveries in the field of magnetic superlattices include the perpendicular anisotropy[2] and the Ruderman-Kittel-Kasuya-Yosida (RKKY)–type oscillatory exchange coupling between magnetic metal layers through nonmagnetic layers. The interlayer exchange coupling has been universally observed in many transition-metal[3] and rare-earth-metal[4] systems. For these studies high-quality well-characterized samples are required since the magnetic properties are quite sensitive to the structural parameters such as layer thickness, epitaxial strains, and interfacial roughness.

Stabilization of metastable magnetic phases in metal multilayers is another highly interesting topic. For example, thin fcc-Fe layers may be stabilized in Fe/Cu(001) superlattices. Because the lattice constant of fcc-Fe on Cu substrates is in the critical region for spin-volume fluctuations, both high-spin (ferromagnetic) and low-spin (antiferromagnetic) states can be obtained depending on the growth temperature which appears to control the tetragonal distortion of fcc-Fe.[5] Furthermore, metastable bcc-Cu (Ref. 6), bcc-Ni (Ref. 7), and hexagonal Fe (Ref. 8) have been reported. These metastable phases are particularly interesting since they are not known in the bulk phase diagram, or they exist only at extremely high pressures or temperatures.

For similar reasons bcc-Co has attracted much attention in the past and was intensively studied by several groups. Bulk Co has a hcp structure at room temperature, while a fcc structure is stable above 410 °C.[9] The bcc phase of Co was grown for the first time on GaAs(110) substrates up to a thickness of t_{Co} =357 Å.[10] The bcc structure was confirmed by electron diffraction, x-ray absorption, and nuclear magnetic resonance (NMR) experiments. It was thought that Co could also be stabilized in the bcc phase within Co/Cr superlattices. However the situation concerning Co/Cr multilayers remains controversial. The first report on a "new" phase within polycrystalline Co/Cr multilayers was published by Walmsley and co-workers.[11] Several years later, Sato[12] reported, however, the absence of a bcc phase in his high-quality sputtered Co/Cr(110) superlattices. Instead he observed the hcp phase of Cr. A further support for the absence of the bcc phase came from Stearns and co-workers[13] who studied sputtered Co/Cr multilayers and pointed out that the first report by Walmsley[11] is questionable because of the misinterpretation of their x-ray diffraction data. Meanwhile in another study of sputtered Co/Cr(110) multilayers a metastable bcc-Co phase for $t_{Co}<15$ Å was reported again.[14] Finally, in a most recent structural study of molecular-beam epitaxy (MBE) grown Co/Cr(110) superlattices no evidence for bcc-Co was found. Instead the presence of the close packed structure of Cr was confirmed,[15] in agreement with the pioneering work of Sato.[12]

In most cases polycrystalline or (110)-oriented Co/Cr multilayers have been studied. This orientation, namely hcp-Co(00.1) or fcc-Co(111) || Cr(110), does not present difficulties in the sample preparation because each

growth plane is most densely packed and therefore stable. Indeed to the best of our knowledge, no (001)-oriented Co/Cr superlattice has been grown so far. A recent low energy electron diffraction (LEED) and Auger electron spectroscopy study of ultrathin Co films on Cr(001) single crystal surfaces showed that there was no change in the LEED pattern up to 20 monolayers (ML's), hence the epitaxial growth of bcc-Co was concluded.[16] However this result appeared not to be reproducible, since a subsequent paper by the same group reported the stabilization of only 1 ML bcc-Co.[17]

The magnetic properties of (001)-oriented Co/Cr superlattices are highly interesting since a strong interlayer exchange coupling is expected: From the intensive studies of Fe/Cr(001) multilayers, Cr(001) is known to mediate a strong exchange interaction with ferromagnetic (FM), antiferromagnetic (AFM), and biquadratic contributions.[18] Many theoretical calculations[19] have been carried out in order to elucidate the electronic and spin structure in Co/Cr(001) superlattices in comparison to Fe/Cr(001).

Recently we have successfully grown high-quality epitaxial Co/Cr(001) superlattices by MBE methods.[20] Magneto-optical studies[21] show that the Co spins exhibit a very strong perpendicular anisotropy with critical film thickness of about 14 Å. The perpendicularly magnetized Co layers show oscillatory exchange coupling. X-ray-scattering experiments along the growth direction indicated that the Co layers exhibit a precursive martensitic phase transition in from hcp to bcc phase with decreasing t_{Co}.[20]

In this paper we focus on the structural properties, especially on the precursive phase transition of Co layers in Co/Cr(001) superlattices. We report experimental evidence for the structural phase transition studied by means of grazing-incidence x-ray-scattering (GIXS) experiments. The paper is organized as follows. In Sec. II we will describe sample preparation techniques and details of the grazing-incidence x-ray-scattering experiments. In Sec. III the results of the in-plane diffraction pattern, in-plane lattice constants, the order parameter measurements, and the out-of-plane d spacing will be described. In Sec. IV the structural properties of Co/Cr(001) will be discussed and compared to other studies. Conclusions are provided in Sec. V.

II. EXPERIMENTAL TECHNIQUES

A. Sample preparation

All samples were prepared in a conventional MBE chamber (RIBER, EVA32) designed for metal epitaxial growth. High-quality sapphire $Al_2O_3(1\bar{1}02)$ substrates were rinsed in acetone and isopropanol, then annealed at 500 °C for 1 h and sputtered with Ar^+ (600 eV, $1\mu A/cm^2$) for 30 min in the introduction chamber. Afterwards the substrate crystals were annealed again at 1100 °C in the preparation chamber which was evacuated by ion pumps and a He cryopump below the base pressure of 4×10^{-9} Pa. During sample growth the pressure was less than 6×10^{-9} Pa. The quality of the clean $Al_2O_3(1\bar{1}02)$ surface was confirmed by sharp streaks and Kikuchi lines observed in reflection high energy electron diffraction (RHEED) experiments. In addition the Auger spectra did not show any detectable impurity on the substrate surfaces. A 500 Å Nb buffer layer then was evaporated on the sapphire substrates at a substrate temperature of 900 °C. On the Nb buffer layer the first Cr layer was grown as thick as 500 Å at 450 °C and annealed at 750 °C. The deposition was continued by the growth of a Co/Cr superlattice at 300~ 350 °C with deposition rates of typically 25 Å/min. The growth on ceramic substrates avoids the problems connected with the cleaning of Cr single crystal surfaces. Co was evaporated by an electron beam gun with an optical deposition controller whereas a Knudsen cell was used for the Cr evaporation. The thicknesses of the Co and Cr layers, t_{Co} and t_{Cr}, respectively, ranged from 5~70 Å with the number of double layers $N = 10 \sim 100$. The layer thicknesses have been confirmed by x-ray small angle reflectivity measurements and x-ray fluorescence analysis using a scanning electron microscope. The Co/Cr(001) superlattices studied here had roughly the same layer thicknesses t_{Co} and t_{Cr}. The interfacial roughness determined by small angle x-ray reflectivity measurements was typically 5 Å.

Figure 1 shows the RHEED patterns from (a) a 20 Å Co layer and (b) a 30 Å Cr layer after the deposition of

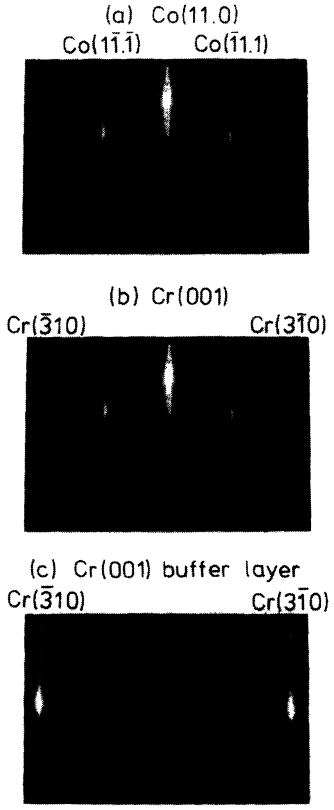

FIG. 1. The RHEED picture from (a) a 20 Å Co layer, (b) a 30 Å Cr layer after the deposition of ten superlattice periods, and (c) the Cr buffer layer with the electron beam in the same azimuth, namely, the scattering vector is parallel to the Co$[\bar{1}1.1]$ and Cr$[3\bar{1}0]$, respectively.

ten superlattice periods with the electron beam in the same azimuth. Both layers exhibit sharp streaks which indicate atomically flat surfaces. We observed RHEED oscillations up to a Co layer thickness of at least 20 ML's. The streaks at the half order wave number of Cr are due to the hcp symmetry of Co. Details about the structure of Co layers will be discussed further below. As one can recognize by comparing the RHEED pattern from the uppermost Cr layer to the one from (c) the Cr buffer layer, the Cr RHEED pattern shows no change during the evaporation of the entire film. This also implies that the truncated structure of each Cr film before depositing Co is always the same for subsequent Co/Cr interfaces and identical to the one of the bulk Cr(001) plane.

B. Grazing incidence x-ray-scattering techniques

We have determined in-plane structural parameters by means of grazing-incidence x-ray-scattering techniques which provide high surface sensitivity together with depth resolved information.[22] The schematic viewgraph of the scattering geometry is shown in Fig. 2. A Mo target in point focus arrangement from an 18 kW rotating anode x-ray generator was used. A flat graphite (002) monochromator and a pair of slits provided a vertical divergence of the primary beam of less than 0.04°. The beam size was $0.3(\mathrm{v})\times5(\mathrm{H})$ mm^2 at the sample position.

The penetration depth of the x rays is controlled by the incident and takeoff angles with respect to the sample surface, α_i and α_f, respectively. In our setup α_i is adjusted by tilting the sample surface against the horizontal plane containing the primary beam, while the scattered x rays are integrated over a range of exit angles α_f's. In most of our experiments α_i was fixed at 0.2 °, yielding a penetration depth Λ of about 500 Å by taking into account the divergence of the primary beam. This penetration depth was chosen to be comparable with the total film thickness of the Co/Cr superlattices. Thus structural information is gathered from the entire superlattice while eliminating background noise from substrate crystals.

The scattering profiles are measured along the longitudinal and transverse directions by $2\theta/\theta$ (radial or longitudinal) and θ (transverse or rocking) scans, respectively. With use of a solar slit of 0.15° horizontal divergence the longitudinal and transverse resolutions were about 0.23° and 0.10°, respectively. The order parameter measurements were carried out by rocking scans of the Co$\{\bar{1}1.1\}$ reflections without the solar slit in the beam path in order to get better statistics for the intensity measurements.

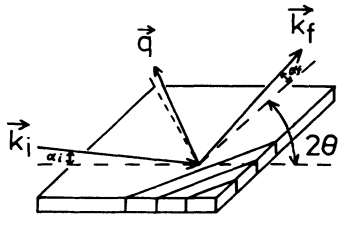

FIG. 2. The schematic outline of the scattering geometry of our grazing-incidence x-ray-scattering experiments.

All measurements were carried out under normal atmospheric conditions and at room temperature.

III. RESULTS

A. In-plane diffraction pattern

Figure 3 summarizes the in-plane diffraction spots from Co/Cr(001) superlattices observed by GIXS experiments. The Cr{110}, Cr{200}, and Cr{220} reflections, denoted by closed circles, are clearly visible at the expected positions for the bcc-Cr(001) plane. In addition, we observe spots which appear at central positions of the Cr reciprocal lattice as shown by open circles and triangles. We have confirmed that these additional spots are due to Co layers since they are not present in single Cr(100) layers. Exactly the same results are obtained from *in situ* RHEED experiments during sample growth. Again bcc reflections appear from the Cr(001) planes, but whenever Co is deposited weak half order spots are seen in addition to strong spots at the same positions as for the Cr layers (see Fig. 1).

In order to understand the observed in-plane diffraction pattern, we compare the experimental results with the pattern expected for hcp-Co(11.0) and fcc-Co(110) planes. This is reasonable since we have shown in our previous paper that the measured out-of-plane lattice spacings $d = 1.26 \sim 1.32$ Å (Ref. 20) are consistent with the d spacing ($d = 1.253$ Å) (Ref. 23) for both the hcp-(11.0) and fcc-(110) planes. The bcc- and fcc-Co(001) planes are ruled out since the out-of-plane d spacings, d=1.41 Å (Ref. 10) and d =1.77 Å, respectively, lie beyond the experimental error. The in-plane diffraction pattern can now completely be accounted for by reflections from the hcp-Co(11.0) plane if the c axis of hcp-Co is assumed to be parallel to the Cr[110] axis. The resulting epitaxial relation can be described as follows:

$$\begin{aligned} &\text{hcp-Co}\,(11.0)\parallel\text{bcc-Cr}\,(001)\ , \\ &\text{hcp-Co}\,[00.1]\parallel\text{bcc-Cr}\,[110]\,. \end{aligned} \tag{1}$$

With this epitaxial relation all observed Bragg peaks can

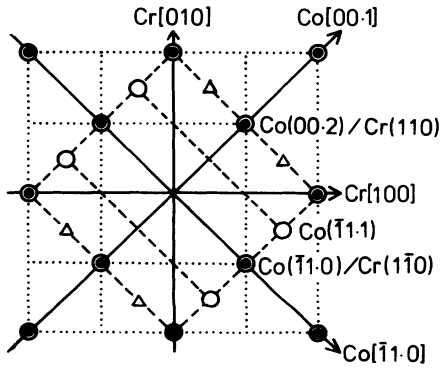

FIG. 3. The observed in-plane diffraction spots. The open circles and triangles denote the reflections from Co layers, while closed circles indicate the ones from Cr layers. The reciprocal lattice of Co and Cr is shown by broken and dotted lines, respectively.

be explained and there are no predicted reflections which cannot be observed. Hence it is confirmed that the hcp-Co(11.0) planes grow epitaxially on Cr(001). According to the orientational relationship in Eq. (1) the reflections have the indices as shown in Fig. 3. The spots denoted by open triangles are explained by Co$\{\bar{1}1.1\}$ reflections from twins whose c axis is parallel to the Cr$[\bar{1}10]$ axis. The epitaxial relation of Co/Cr(001) mentioned above is equivalent to the Pitsch-Schrader orientational relationship.[24] This orientation has been predicted from geometrical considerations to be most favorable for Co on Cr(001),[25] and in fact has been observed by an electron diffraction study of 1000 Å thick Co films on Cr(001).[26] Our present result agrees with these two studies. The possibility of having fcc-Co(110) planes on Cr(001) was ruled out by the difference in the size of the in-plane unit cells. The fcc-Co(110) plane has an ABC stacking along the $[\bar{1}11]$ direction, whereas hcp-Co(11.0) has an AB stacking along the [00.1] direction. Our data are consistent with the AB stacking sequence.

B. The crystal structure

Figure 4 shows the crystal structure of hcp-Co(11.0) (open circles) on bcc-Cr(001) (dark circles) which satisfies the epitaxial relation described above. It is clearly seen that the Co(11.0) plane fits well on Cr(001), indicating the stability of this growth orientation. The cross sectional view of this superlattice illustrates the similarity of the local symmetry of the Co(00.1) basal plane to the one of Cr(110) as shown in Fig. 4(b), implying again the stability of this structure. The misfit between Co and Cr in-plane unit cells can be calculated as follows:

$$\frac{c_{\mathrm{Co}} - \sqrt{2}a_{\mathrm{Cr}}}{\sqrt{2}a_{\mathrm{Cr}}} = -0.2\% \,(\|\mathrm{Co}\,[00.1])\ ,$$
$$\frac{\sqrt{3}a_{\mathrm{Co}} - \sqrt{2}a_{\mathrm{Cr}}}{\sqrt{2}a_{\mathrm{Cr}}} = 6.4\% \left(\|\mathrm{Co}\,[\bar{1}1.0]\right), \tag{2}$$

where $a_{\mathrm{Co}} = 2.507$ Å, $c_{\mathrm{Co}} = 4.070$ Å, and $a_{\mathrm{Cr}} = 2.885$ Å are the bulk lattice constants of Co and Cr, respectively.[23] It should be noted that the Co lattice in Fig. 4 has been distorted in order to show no lattice mismatch.

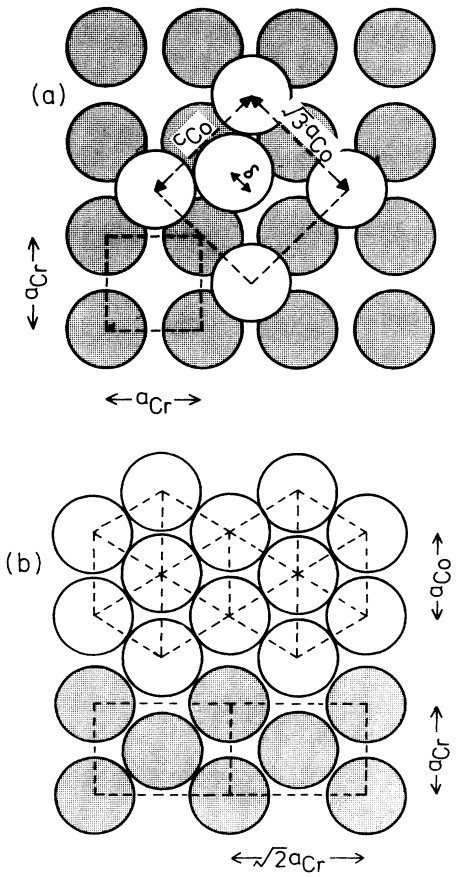

FIG. 4. The crystal structure of Co/Cr superlattices. The white and dark circles indicate Co and Cr atoms, respectively. (a) Top view. The broken lines indicate the size of the in-plane unit cell. (b) Cross sectional viewgraph of a Co/Cr(001) superlattice parallel to the Co(00.1) basal plane.

The crystal structure of the Co/Cr(001) superlattices leads us to a very interesting insight concerning the stability of bcc-Co. As shown in Fig. 4 the position of the Co center atoms is displaced by an amount δ from the hollow sites (bcc sites) on the Cr(001) surface, assuming that the Co corner atoms are placed on hollow sites. It can be easily imagined that the surface potential of Cr(001) has a minimum on the hollow sites, such that any displacement of an adsorbate Co atom away from this site would result in an energy increase. This will certainly contribute to the instability of the hcp-Co structure for very thin Co layers on Cr(001). In fact, it would be more reasonable to assume that within the first monolayer the Co atoms on Cr(100) would occupy all the hollow sites and assume therefore a bcc structure. For increasing t_{Co} the hcp structure is expected to be more stable since, after all, it is the ground state of bulk Co. As a consequence of the competition between the surface potential of Cr(001) and the bulk potential of Co we can expect that Co layers exhibit a hcp to bcc structural phase transition with decreasing t_{Co}. Furthermore, the hcp $\leftrightarrow$ bcc structural phase transition can be described by the displacement δ as the order parameter of the transition, where δ=0(1) corresponds to bcc(hcp) structure. The order parameter, in turn, can be determined by means of intensity measurements I of the hcp reciprocal lattice points $\{\bar{1}1.1\}$

$$I\{\bar{1}1.1\} = 4f_{\mathrm{Co}}^2 \left(\sin\frac{\pi}{3}\delta\right)^2 \propto \delta^2\ , \tag{3}$$

where f_{Co} is the atomic form factor of Co atoms. The experimental result of the order parameter measurements will be reported in Sec. III D.

C. In-plane scattering profiles and lattice constants

Representative spectra of in-plane radial scans through the Cr(110) peak are shown in Fig. 5. For the rather large Co thickness of $t_{\mathrm{Co}} = 44.7$ Å, the Co$(\bar{1}1.0)$ and Cr(110) peaks coexist at almost their respective bulk positions. With decreasing Co layer thickness, the Co$(\bar{1}1.0)$ peak shifts towards the Cr(110) peak, and for $t_{\mathrm{Co}} = 12.9$ Å

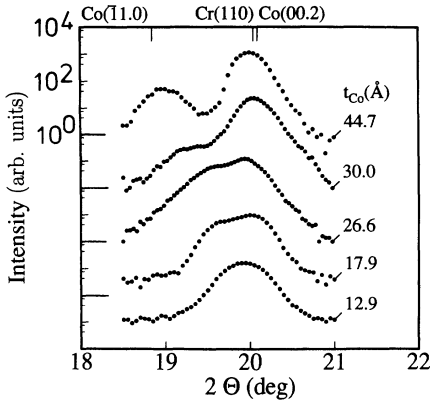

FIG. 5. The t_{Co} dependence of the scattering profile observed by the in-plane radial scan around the Cr(110) peak.

both peaks cannot be resolved any more within the experimental resolution. Meanwhile, there is no splitting of the Co(00.2) peak to be observed for the entire thickness range t_{Co} studied here. The Co(00.2) peak could be traced in the same radial scan as shown in Fig. 5 because of the twin structure occurring in the Co layers. Along the [00.1] direction the Co layers appear to be commensurate with the Cr substrate because of the very small lattice misfit of only about 0.2% along this direction. From these results we can conclude that the Co layers in Co/Cr(001) superlattices exhibit a one-dimensional lattice relaxation only along the Co$[\bar{1}1.0]$ axis. The small in-plane mosaic spread of about 0.3° is proof of the high quality of our samples. The in-plane crystallographic coherence length estimated by the linewidths of the radial scan was typically 100 Å.

The one-dimensional lattice relaxation can also be recognized by the shift of the Co$\{\bar{1}1.1\}$ peak position as shown in Fig. 6. By carrying out rocking scans as well as radial scans we can determine the reciprocal lattice vectors $\mathbf{q}\{\bar{1}1.1\}$ in the reciprocal space. According to the following relations the reciprocal lattice vectors $\mathbf{q}(00.1)$ and $\mathbf{q}(\bar{1}1.0)$, and hence the in-plane lattice constants of

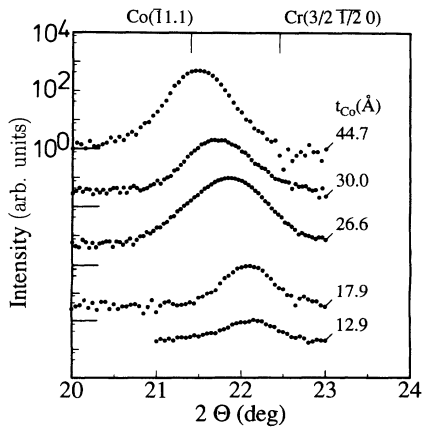

FIG. 6. The t_{Co} dependence of the scattering profile observed by the in-plane radial scan around the Co$\{\bar{1}1.1\}$ spots.

Co, c_{Co}, and $2d(\bar{1}1.0)$, can be determined as follows:

$$\mathbf{q}(00.1) = [\mathbf{q}(\bar{1}1.1) - \mathbf{q}(\bar{1}1.\bar{1})]/2\,,$$
$$\mathbf{q}(\bar{1}1.0) = [\mathbf{q}(\bar{1}1.1) - \mathbf{q}(1\bar{1}.1)]/2\,. \tag{4}$$

The Co in-plane lattice constants are shown in Fig. 7 as a function of t_{Co}. The Co in-plane lattice constant $2d(\bar{1}1.0)$ exhibits a significant change from the bulk value to the epitaxial value of $\sqrt{2}a_{Cr}$ with decreasing t_{Co}. Over the same thickness range c_{Co} remains constant and is in good agreement with the bulk and/or epitaxial value of $\sqrt{2}a_{Cr}$. As also shown in Fig. 7, the Cr in-plane lattice parameter a_{Cr} exhibits no significant change for t_{Cr} =10–50 Å, indicating a remarkable stability of the Cr lattice.

Since c_{Co} is constant and almost equal to $\sqrt{2}a_{Cr}$, the deviation of $2d(\bar{1}1.0)$ from $\sqrt{2}a_{Cr}$ measures the squareness of the Co in-plane unit cell. The observed one-dimensional relaxation implies that the Co in-plane unit cell changes its shape from rectangular (hcp) to square (bcc) with decreasing t_{Co}. This can be taken as one of the experimental manifestations for the bcc↔hcp structural phase transition of Co layers in Co/Cr(001) superlattices.

D. Order parameter measurements

Figure 8 shows the t_{Co} dependence of the integrated hcp-Co$\{\bar{1}1.1\}$ peak intensity measured by both GIXS (crosses) and by *in situ* RHEED (closed circles). Both intensities are normalized by their saturation intensities. The two scattering techniques sample different depths. The RHEED experiment is highly surface sensitive, so that only 1–2 surface atomic layers can be observed, while in the GIXS experiment the intensity is averaged over the entire film thickness. In order to compare the GIXS data with the RHEED results the x-ray-scattering intensities

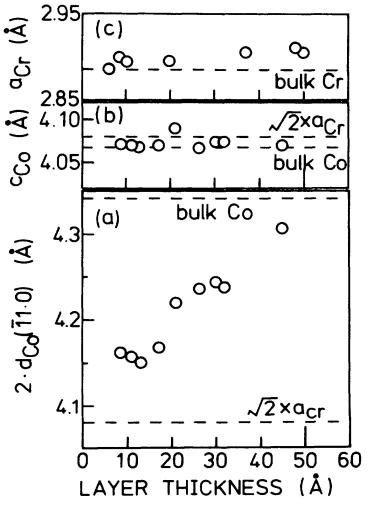

FIG. 7. The layer thickness dependence of the in-plane Co lattice constants $2d_{Co}(\bar{1}1.0)$, c_{Co}, and the one of Cr, a_{Cr}. In this figure Co lattice constants are plotted as a function of t_{Co} while a_{Cr} is plotted vs t_{Cr}.

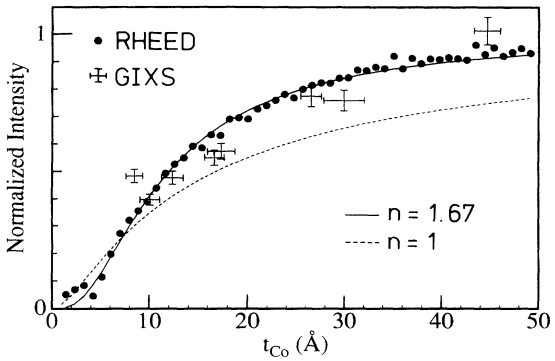

FIG. 8. The t_{Co}-dependence of the intensity I of the *hcp* spots Co$\{\bar{1}1.1\}$. The circles and the crosses indicate the experimental results from the RHEED and the grazing-incidence x-ray-scattering experiments, respectively. The solid and the broken lines show the fitting and for an ideal case with $n = 1$.

are normalized by the effective Co layer thickness $\tilde{t}_{Co}$ as follows:[27]

$$\tilde{t}_{Co} = \frac{t_{Co}}{t_{Co}+t_{Cr}} \int_0^{N(t_{Co}+t_{Cr})} e^{-\frac{t}{\Lambda}} dt = \frac{t_{Co}\cdot\Lambda}{t_{Co}+t_{Cr}} \left\{1 - \exp\left[-\frac{N(t_{Co}+t_{Cr})}{\Lambda}\right]\right\}. \quad (5)$$

Here Λ is the penetration depth of x rays described in Sec. II B and N is the number of double layers, hence $N(t_{Co}+t_{Cr})$ is the thickness of the superlattices. The x-ray data show the average scattering intensities per Co atomic layer.

The intensities from the x-ray and RHEED experiments are in quite good agreement and decrease rapidly with decreasing t_{Co}. As described in Sec. III B, the Co$\{\bar{1}1.1\}$ reflections are due to the hcp symmetry and the intensity is proportional to the square of the order parameter δ. δ, in turn, is the displacement of the Co atoms from the hollow bcc sites, with $\delta = 0\,(1)$ corresponding to the bcc(hcp) phase, respectively. Therefore, the observed continuous change of I is a further clear sign for the Co layers in Co/Cr(001) superlattices undergoing a structural phase transition from hcp to bcc with decreasing t_{Co}. It should be noted that the continuous change of the intensity in a wide region of t_{Co} up to 70 Å cannot be due to the effect of the alloying layer which might be formed at the interfaces, because the thickness of the alloying layer is expected to be very small; the thickness is less than the total roughness of about 5 Å which is determined by small angle x-ray reflectivity measurements. As shown in Fig. 8 and by the RHEED line scans (Fig. 5 in Ref. 20), very weak but clearly visible Co$\{\bar{1}1.1\}$ spots are observable for t_{Co} down to 4 Å, indicating that the hcp symmetry remains even for these thin Co layers. The good agreement between RHEED and GIXS data implies that the order parameter is more or less homogeneous throughout the layer thickness.

We have carried out a simple model calculation to explain the t_{Co} dependence of the order parameter $\delta\,(t_{Co})$. The total energy E (per Co atom) which is responsible for the crystal structure of the Co layers can be described as a sum of interfacial and bulk contributions

$$E = \left(\frac{1}{t_{Co}}\right)^n \frac{1}{2}k_i\delta^2 + \frac{1}{2}k_v\,(1-\delta)^2\ , \quad (6)$$

where k_i and k_v are the effective force constants for the interfacial and bulk potentials, respectively. The interfacial contribution (the first term) has the same periodicity as the bcc-Cr lattice and has a minimum at the hollow sites of Cr(001), i.e., at δ=0 as shown in Fig. 4. At the same time the competing bulk contribution (the second term) tends to stabilize the hcp structure (δ=1). In Eq. (6) we assume complete uniformity of the order parameter within a Co layer, which is supported by the experimental results as described before. The power n of t_{Co} is a parameter which controls the strength of the interfacial contribution. In an ideal case n=1 is expected. The strain energy due to the epitaxial misfit has been neglected, since static strain affects only the unit cell deformation but cannot cause local displacements of Co center atoms as shown in Fig. 4(a). The minimum of E is found by taking the derivative with respect to δ, yielding

$$\delta\,(t_{Co}) = \frac{t_{Co}^n}{a + t_{Co}^n}, \quad (7)$$

where $a = k_i/k_v$. The solid line in Fig. 8 represents a fit of the expression $I = \delta^2$ to the data points, where δ is given by Eq. (7). The experimental data are described rather well with the fitting parameters n=1.67 and a=26.5. The broken line in Fig. 8 is the calculated intensity assuming the ideal values n=1 and a=6.5,[28] which is clearly not in agreement with the experimental results. This discrepancy can be qualitatively understood in terms of the relaxation of the Co lattice as described in Sec. III C. The lattice mismatch causes the interfacial contribution to the total energy to be weaker than the expected t_{Co}^{-1} dependence. Thus n=1.67 may be quite reasonable. As concerns the parameter a, there is at present no experimental or theoretical study available with which this parameter could be compared.

E. Out-of-plane *d* spacing

Figure 9 shows the experimental results of the out-of-plane d spacing of the Co layers $d\,(11.0)$ in Co/Cr(001) superlattices published in our previous paper.[20] At that time we remarked the striking out-of-plane expansion but were unable to provide an explanation. With the in-plane data on hand, we can shed some light on the Co layer expansion with decreasing t_{Co}. The out-of-plane expansion cannot be explained by the usual Poisson response e_2 due to the in-plane strain of the Co layers on Cr(001), which is given by

$$e_2 = -\frac{1}{c_{11}}\,(c_{12}e_1 + c_{13}e_3)\,, \quad (8)$$

where $c_{11} = 3.07 \times 10^{11}$ N/m^2, $c_{12} = 1.65 \times 10^{11}$ N/m^2, and $c_{13} = 1.03 \times 10^{11}$ N/m^2 are the elastic constants of bulk hcp-Co,[29] e_1 and e_3 are the in-plane strains along the Co$[\bar{1}1.0]$ and Co[00.1] axis, respectively. The broken

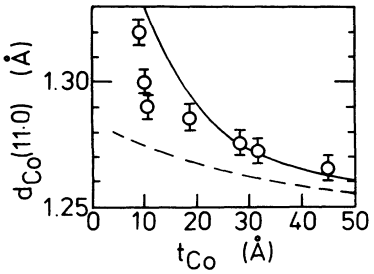

FIG. 9. The t_{Co} dependence of the out-of-plane d spacing, $d(11.0)$. The open circles are the experimental data published in Ref. 20. The solid line is the calculated d spacing from a rigid-atom model assuming the hcp-bcc structural transition of the Co layers. The broken line shows the expected one from Poisson expansion calculated from the observed epitaxial strains and bulk elastic constants.

line in Fig. 9 is the calculated $d(11.0)$ spacing as expected from the Poisson response e_2 according to Eq. (8) and the use of the measured in-plane strains reported in this study (Sec. III C). Obviously the broken line cannot explain the experimental results.

The observed out-of-plane d spacing can, however, be accounted for quite well by a very simple rigid atom model. From geometrical considerations we get

$$d(11.0) = \sqrt{(2r)^2 - \left(\frac{c_{Co}}{2}\right)^2 - \left(\frac{a_{Co}}{2\sqrt{3}}\right)^2 \delta^2}, \qquad (9)$$

where r is the atomic radius of Co.[30] The solid line in Fig. 9 is the calculated d-spacing from the rigid atom model using the experimental results for the order parameter measurements in this paper (Fig. 8). It is evident that the rigid-atom model can much better describe the out-of-plane expansion of the Co layers in Co/Cr(100) superlattices than the Poisson model. The small deviation from the experimental data noticed for thin Co layers is most likely due to the oversimplification of the rigid-atom model. Nevertheless, from the present results it is now clear that the previously observed anomalous out-of-plane expansion can be explained as a precursive response to the bcc $\leftrightarrow$ hcp structural phase transition of Co layers in Co/Cr(001) superlattices.

IV. DISCUSSION

The structural properties of Co/Cr(001) superlattices are quite unique and therefore very interesting in comparison to other superlattices. In the present case hcp-Co(11.0) which exhibits in-plane twofold symmetry is grown on bcc-Cr(001) which has a cubic symmetry. Therefore the in-plane symmetry changes from twofold to fourfold, associated with the hcp to bcc phase transition of the Co layers. In contrast, the in-plane symmetry in many other metastable systems is conserved and remains the same throughout the structural transition, and usually is also identical to the symmetry of the second component in the superlattices. For example the in-plane fourfold symmetry in (001)-oriented superlattices with bct (fct) layer structures is conserved with respect to the parent bcc or fcc phases. In another example the sixfold symmetry is conserved in (111)-oriented superlattices containing fcc(111) and hcp(00.1) layers. In those cases the structural phase transition can be described by the out-of-plane structural properties along the growth direction such as the tetragonal distortion or the layer stacking sequence. Superlattices with alternating bcc(110) and fcc(111) or hcp (001) layers with Nishiyama-Wasserman or Kurdjumov-Sachs orientation might be similar to Co/Cr(001) because of the mismatch of the in-plane symmetry. However, in most of those superlattices a homogeneous and static lattice distortion due to the large lattice mismatch between bcc(110) and fcc(111) or hcp(00.1) seems to be more important than the in-plane local atomic displacement observed in the Co/Cr(001) system.

Induced strains which are not explained by elastic theories are recently of high interest. A non-Poisson-type behavior has been observed in many metal multilayers composed of noble and transition metals such as Au/Ni,[31] Mo/Ni,[32] and Cu/Nb,[33] etc. This behavior is often associated with the so-called super modulus effect, implying an anomalous hardening of the elastic constants beyond a rule-of-mixture. A non-Poisson behavior has recently also been observed for thin Cr films on Nb which may be of magnetic origin.[34] On the other hand, recent structural studies of Co/Cu superlattices[35,36] find that the in- and out-of-plane lattice constants can be completely understood within the frame of elastic theories using bulk elastic constants. In this sense Co/Cu superlattices behave quite normally although the metastable fcc structure of Co in these superlattices is actually a proximity effect of Cu.

The results of this study are inconsistent with a recent LEED observation by Scheurer and co-workers.[16] These authors have reported a (1×1) LEED pattern for ultrathin Co films on Cr(001), and they conclude that the metastable bcc-Co phase can be grown layer by layer up to 20 ML (=28 Å for Co in the bcc phase). It should be pointed out that our LEED pattern from a 30 Å thick hcp-Co(11.0) layer on Cr(001) exhibits also a clear (1×1) pattern for scattering vectors $|q| < 3.2$ Å^{-1}, but very weak Co$\{\bar{1}1.1\}$ spots become visible at $|q| = 3.3$ Å^{-1}. At present we have no clear explanation for this discrepancy. It appears, however, from our experience that it would be rather difficult to identify uniquely the crystal structure of Co with LEED experiments, since the hcp-Co$\{\bar{1}1.1\}$ reflections are very weak. Furthermore, from the LEED pattern published in Ref. 16 it appears almost impossible to identify the crystal structure of Co, because the section of the reciprocal space was too small to detect the Co$\{\bar{1}1.1\}$ spots. Grazing-incidence x-ray-scattering experiments which probe the entire Co layer thickness rather than the surface as in LEED, is clearly a more powerful method when it comes to subtleties concerning the in-plane structure of thin films.

V. CONCLUSIONS

We have carried out an extensive study of the structural properties of high-quality Co/Cr(001) superlat-

tices by means of grazing-incidence x-ray-scattering techniques. We find that hcp-Co(11.0) grows epitaxially on Cr(001). The in-plane epitaxial orientation determined is identical to the Pitsch-Schrader relationship. We provide experimental evidence that a precursive bcc $\leftrightarrow$ hcp structural phase transition of the Co layers in Co/Cr(001) superlattice takes place, based on the following observations: (i) the shape of the in-plane unit cell changes from rectangular to nearly square; (ii) the intensity of the hcp Co$\{\bar{1}1.1\}$ peaks, which are forbidden in the bcc structure, shows a continuous decrease, implying an in-plane symmetry change of the Co layers from hcp to bcc with decreasing t_{Co}; (iii) the observed anomalous out-of-plane expansion of the Co layers can be described by a rigid-atom model assuming that the precursive bcc $\leftrightarrow$ hcp structural phase transition takes place.

Fe/Cr and Co/Cr superlattices have in the past often been compared as concerns their perspective magnetic properties. Experimentally this comparison could not be pursued because of the difficulties encountered in growing Co/Cr(001) superlattices. We have now succeeded in the epitaxial growth of single crystalline Co/Cr(001) superlattices and our structural studies presented in this paper indicate that Co/Cr and Fe/Cr exhibit rather different structural properties. We therefore expect the magnetic properties also to reflect this difference. The magnetic properties will be published in a forthcoming paper. A preliminary report can, however, be found in Ref. 21 .

ACKNOWLEDGMENTS

We would like to thank G.A. Prinz, N. Sato, and M.C. Cadeville for the stimulating discussions. We also thank J. Podschwadek and W. Oswald for their technical support. This work was partly supported by the Deutsche Forschungsgemeinschaft (SFB 166) and by the Ministerium für Wissenschaft und Forschung NRW (Germany), which is gratefully acknowledged.

[1]For recent reviews, see *Proceedings of the International Symposium on Magnetic Ultrathin Films, Multilayers, and Surfaces, Lyon, 1992* [J. Magn. Magn. Mater. **121** (1993)]; *Proceedings of the Thirty-seventh Annual Conference on Magnetism and Magnetic Materials* [J. Appl. Phys. **73**, 10 (1993)].

[2]T. Shinjo, Surf. Sci. Rep. **12**, 49 (1991).

[3]S.S.P. Parkin, Phys. Rev. Lett. **67**, 3598 (1991).

[4]C.F. Majkrzak, J. Kwo, M. Hong, Y. Yafet, D. Gibbs, C.L. Chien, and J. Bohr, Adv. Phys. **40**, 99 (1991).

[5]W.A.A. Macedo and W. Keune, Phys. Rev. Lett. **61**, 475 (1988); W.A.A. Macedo, W. Keune, and E.D. Ellerbrock, J. Magn. Magn. Mater. **93**, 552 (1991).

[6]B. Heinrich, Z. Celinski, J.F. Cochran, A.S. Arrott, K. Myrte, and S.T. Purcell, Phys. Rev. B **47**, 5077 (1993).

[7]M.D. Wieczorek, D.J. Keavney, D.F. Storm, and J.C. Walker, J. Magn. Magn. Mater. **121**, 34 (1993), and references cited therein.

[8]M. Maurer, J.C. Ousset, M.F. Ravet, and M. Piecuch, Mat. Res. Soc. Symp. Proc. **87**, 231 (1990).

[9]For example, S.M. Shapiro and S.C. Moss, Phys. Rev. B **15**, 2726 (1977); F. Frey, W. Prandl, J. Schneider, C. Zeyen, and K. Ziebeck, J. Phys. F **9**, 603 (1979).

[10]G.A. Prinz, Phys. Rev. Lett. **54**, 1051 (1985); P.C. Riedi, T. Dumelow, M. Rubinstein, G.A. Prinz, and S.B. Qadri, Phys. Rev. B **36**, 4595 (1987); Y.U. Ydzerda, W.T. Elam, B.T. Jonker, and G.A. Prinz, Phys. Rev. Lett. **62**, 2480 (1989).

[11]R. Walmsley, J. Thompson, D. Friedman, R.M. White, and T.H. Geballe, IEEE Trans. Magn. Magn. **19**, 1992 (1983).

[12]N. Sato, J. Appl. Phys. **61**, 1979 (1987).

[13]M.B. Stearns, C.H. Lee, and T.L. Groy, Phys. Rev. B **40**, 8256 (1989).

[14]P. Boher, F. Giron, Ph. Houdy, P. Beauvillain, C. Chappert, and P. Veillet, J. Appl. Phys. **70**, 5507 (1991).

[15]W. Vavra, D. Barlett, S. Elagoz, C. Uher, and R. Clarke, Phys. Rev. B **47**, 5500 (1993); Y. Henry, C. Mény, A. Dinia, and P. Panissod, *ibid.* **47**, 15 037 (1993).

[16]F. Scheurer, B. Carrière, J.P. Deville, and E. Beaurepaire, Surf. Sci. **245**, L175 (1991).

[17]F. Scheurer, P. Ohresser, B. Carrière, J.P. Deville, R. Baudoing-Savois, and Y. Gauthier, Surf. Sci. **298**, 107 (1993).

[18]J. Unguris, R.J. Celotta, and D.T. Pierce, Phys. Rev. Lett. **67**, 140 (1991); **69**, 1125 (1992); S.T. Purcell, W. Folkerts, M.T. Johnson, N.W.E. McGee, K. Jager, J. aan de Stegge, W.B. Zeper, W. Hoving, and P. Grünberg, *ibid.* **67**, 903 (1991).

[19]F. Herman, P. Lambin, and O. Jepsen, Phys. Rev. B **31**, 4394 (1985); H. Hasegawa and F. Herman, *ibid.* **38**, 4863 (1988); H. Hasegawa, *ibid.* **43**, 10 803 (1991); D. Stoeffler and F. Gautier, *ibid.* **44**, 10 389 (1991); Surf. Sci. **251/252**, 31 (1991).

[20]W. Donner, N. Metoki, A. Abromeit, and H. Zabel, Phys. Rev. B **48**, 14 745 (1993).

[21]N. Metoki, W. Donner, Th. Zeidler, and H. Zabel, J. Magn. Magn. Mater. **126**, 397 (1993); W. Donner, Th. Zeidler, F. Schreiber, N. Metoki, and H. Zabel, J. Appl. Phys. **75**, 8 (1994).

[22]R. Feidenhans'l, Surf. Sci. Rep. **10**, 105 (1989); *Surface X-Ray and Neutron Scattering*, edited by H. Zabel and I.K. Robinson (Springer-Verlag, Berlin, 1992), p. 181ff.

[23]X. Wyckoff, *Crystal Structures*, 2nd ed. (John Wiley & Sons, New York, 1963), Vol. 1, p. 12.

[24]W. Pitsch and A. Schrader, Arch. Eisenhütt Wes. **29**, 715 (1958).

[25]L.A. Bruce and H. Jaeger, Philos. Mag. A **40**, 97 (1979).

[26]J. Daval and D. Randet, IEEE Trans. Mag. **6**, 768 (1970).

[27]This expression is derived by the theoretical calculation for surface scattering geometry with distorted wave approximation [See, for example, H. Dosch, Phys. Rev. B **35**, 2137 (1987)]. Note that in the present case Λ/d is very large ($\Lambda/d \cong 400$).

[28]In the calculation for an ideal case a was chosen so as to get $I=\frac{1}{4}$ at $t_{Co}=a$.

[29]*American Institute of Physics Handbook*, 2nd ed. (McGraw-Hill, New York, 1963).

[30]We changed slightly the lattice constants of Co and Co atomic radius from the known value so as to give a correct out-of-plane d spacing for bcc (hcp) at δ=0(1).

[31] A.F. Jankowski, J. Appl. Phys. **71**, 1782 (1992); J. Chaudhuri, V. Gondhalekar, and A.F. Jankowski, *ibid.* **71**, 3816 (1992); N. Nakayama, L. Wu, H. Dohnomae, T. Shinjo, J. Kim, and C.M. Falco, J. Magn. Magn. Mater. (to be published).

[32] Y. Ohishi *et al.*, in *Multilayers*, edited by M. Doyama *et al.*, MRS Symposia Proceedings No. 10 (Materials Research Society, Pittsburgh, PA, 1989), p. 569; E.E. Fullerton, I.K. Schuller, H. Vanderstraeten, and Y. Bruynseraede, Phys. Phys. Rev. B **45**, 9292 (1992).

[33] A. Fartash, M. Grimsditch, E.F. Fullerton, and I.K. Schuller, Phys. Rev. B **47**, 12 813 (1993).

[34] P. Sonntag, W. Donner, N. Metoki, and H. Zabel, Phys. Rev. B **49**, 2869 (1994).

[35] P. Bödeker, A. Abromeit, K. Bröhl, P. Sonntag, N. Metoki, and H. Zabel, Phys. Rev. B **47**, 2353 (1993).

[36] Ch. Morawe, A. Abromeit, N. Metoki, P. Sonntag, and H. Zabel, J. Mater. Res. (to be published).

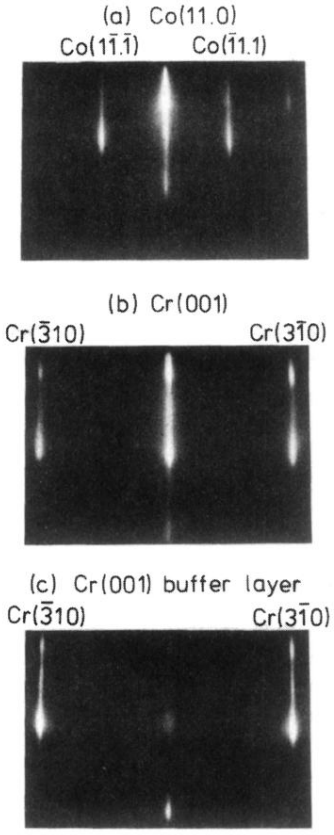

FIG. 1. The RHEED picture from (a) a 20 Å Co layer, (b) a 30 Å Cr layer after the deposition of ten superlattice periods, and (c) the Cr buffer layer with the electron beam in the same azimuth, namely, the scattering vector is parallel to the Co$[\bar{1}1.1]$ and Cr$[3\bar{1}0]$, respectively.

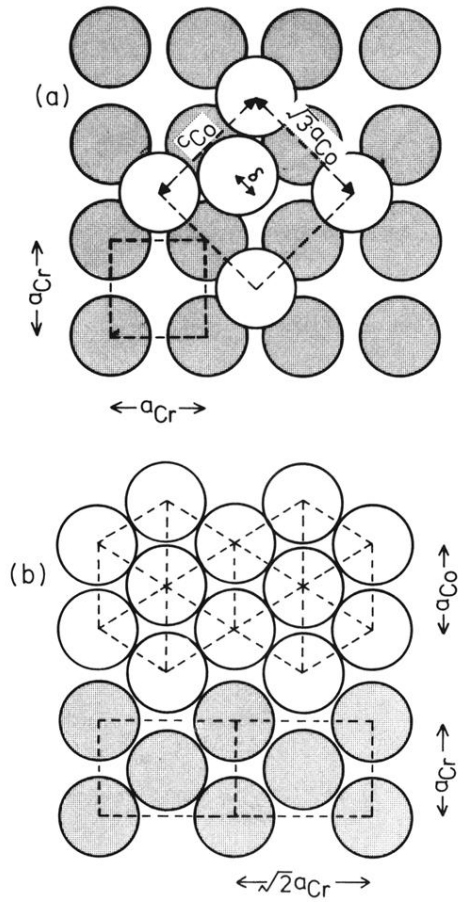

FIG. 4. The crystal structure of Co/Cr superlattices. The white and dark circles indicate Co and Cr atoms, respectively. (a) Top view. The broken lines indicate the size of the in-plane unit cell. (b) Cross sectional viewgraph of a Co/Cr(001) superlattice parallel to the Co(00.1) basal plane.